Diffraction of light in ordered and disordered structures of liquid-crystal blue phases

E. I. Demikhov, V. K. Dolganov, and S. P. Krylova

Institute of Solid State Physics, Academy of Sciences of the USSR, Chernogolovka, Moscow Province
(Submitted 16 April 1987)
Zh. Eksp. Teor. Fiz. **93**, 1750–1756 (November 1987)

An investigation was made of the diffraction of light in three-dimensionally ordered *BP* I and *BP* II phases and in a macroscopically disordered *BP* III phase of cholesteric liquid crystals. The experimental results were compared with the various models of disorder. The diffraction in *BP* III was found to be similar to that in solid glassy structures. The dimensions of unit cells and the parameters representing the disorder of structures with different values of the cholesteric helix pitch were determined.

I. INTRODUCTION

Blue phases of liquid crystals are attracting much attention.[1,2] These phases are exhibited by the majority of chiral liquid crystals. It has been established that the blue phases *BP* I and *BP* II have a three-dimensional periodic structure which is in many respects analogous to crystalline structures. The sequence of the phase transitions between the blue phases and their number are determined by the pitch of the cholesteric helix. The most interesting results are obtained when the pitch is small and one substance exhibits three blue phases (*BP* I, *BP* II, *BP* III). It has been shown experimentally and theoretically that *BP* I and *BP* II form the bcc and simple cubic cells with a macroscopic long-range translational order of the orientations of the molecules and a structure period 100-400 nm.[3–5] The nature of molecular ordering in the *BP* III phase ("fog" phase) at distances comparable with the effective period is not yet clear. The transmission spectra[3] and the rotation of the plane of polarization of light[6,7] in *BP* III indicate structural ordering of the chiral type. The wide-band diffraction of light in *BP* III reported in Ref. 8 suggests disorder. However, the available experimental data on the fog phase are insufficient for a complete description of its structural features.

We report measurements of the diffraction of visible and ultraviolet light in mixtures of chiral liquid crystals with different sizes of the unit cell. We compare the experimental data with various models of disorder. We demonstrate similarity between the diffraction in the fog phase of liquid crystals and solid-state amorphous structures.

II. EXPERIMENTAL RESULTS

Measurements were carried out on *BP* I, *BP* II, and *BP* III and on the cholesteric phase of mixtures of cholesteryl nonanoate (CN) and cholesteryl chloride (CC) in the range of CC concentrations from zero to 14 wt.%; some measurements were also made on pure CC. The CN and CC molecules have different signs of the chirality, so that by increasing the concentration of one component we could alter the helix pitch. The diffraction was measured at a fixed scattering angle ($2\theta = 170°$) in the scattered-wavelength range $\lambda = 650$–300 nm. Planar liquid crystal samples were in cells with a gap of 200–500 μ and the diffraction was recorded from a part of a sample of ~ 0.3 mm transverse size and temperatures in a thermostat were kept constant to within ~ 0.01 °C.

Figure 1 shows a typical diffraction pattern of the phases *BP* I, *BP* II, and *BP* III. The diffraction due to different planes of cubic *BP* I and *BP* II structures [for example, the (110), (200), and (211) planes in *BP* I] was determined employing polydomain samples formed in quartz cells without any special treatment with surfactants. Preparation of *BP* I by heating the cholesteric phase usually produced a polycrystalline sample with fairly small domains. Cooling from the isotropic phase gave rise to single crystals of size in excess of 20 μ. In this case the relative intensities of the reflections were determined by the distribution of the orientations of single crystals and could differ from sample to sample. The pattern of diffraction in *BP* III depended on the method used to prepare this phase. The temperature dependences of the positions of the diffraction lines in the spectrum obtained for a mixture of the CN:CC = 90:10 composition was of the type shown in Fig. 2. Similar temperature dependences were obtained also for other structures. A good agreement was observed between the experimental positions of the short-wavelength diffraction lines (at ~ 400 and ~ 340 nm for *BP* I and at 340 nm for *BP* II) and the wavelengths of the (200), (211), and (110) reflections deduced from the positions of the long-wavelength diffraction lines (~ 570 nm for *BP* I and 470 nm for *BP* II) (Fig. 2). The dependence of the spectral position λ_B of the diffraction lines (110) and (100) of the cubic phases *BP* I and *BP* II on the wavelength of the selective reflection λ_C in the cholesteric phase had the form shown in Fig. 3a. In the case of *BP* I and *BP* II and for the cholesteric

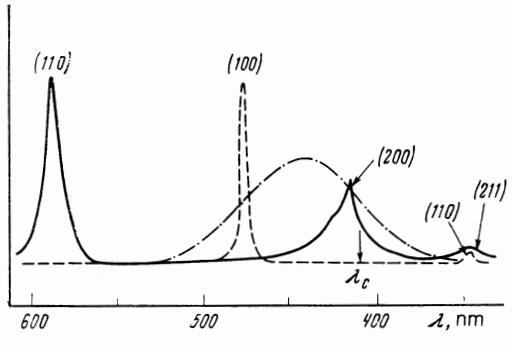

FIG. 1. Spectrum of light diffracted by a CN-CC mixture (90:10) in the phases *BP* I ($T = 85.97$ °C, continuous curve), *BP* II ($T = 86.23$ °C, dashed curve), and *BP* III ($T = 86.33°$, chain curve).

 0038-5646/87/110998-04$04.00

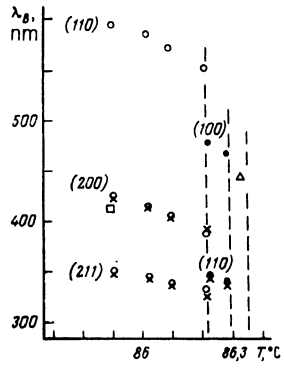

FIG. 2. Temperature dependences of the positions of reflections exhibited by the phases *BP* I (○), *BP* II (●), and *BP* III (△), and by the cholesteric CN-CC (90:10) phase; □ denotes λ_C and × denotes the positions of the reflections deduced from the long-wavelength diffraction lines: $\lambda_B^{(200)} = \lambda_B^{(110)}/2^{1/2}$, $\lambda_B^{(211)} = \lambda_B^{(110)}/3^{1/2}$ (*BP* I); $\lambda_B^{(110)} = \lambda_B^{(100)}/2^{1/2}$ (*BP* II).

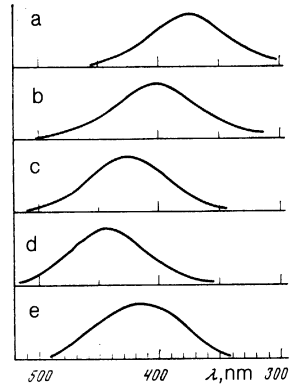

FIG. 4. Spectra of wide-band diffraction in *BP* III observed for the following samples: a) CN; b) CN-CC (95:5); c) CN-CC (93:7); d) CN-CC (90:10); e) CC.

phase we determined the selective reflection wavelengths at a temperature close to the transition to the higher-temperature phase. We included in this figure also the corresponding data on the position of the maximum of the wide-band diffraction λ_B of the fog phase. In samples characterized by $\lambda_C > 440$ nm we did not observe the fog phase. In the case of CN, CC, and CN-CC mixtures forming the fog phase we determined the wide-band diffraction of *BP* III, plotted in Fig. 4.

III. DISCUSSION

The investigated structures exhibited a linear dependence of the size of the cubic cell on the pitch of the cholesteric helix (Fig. 3a). The ratio λ_B/λ_C (Fig. 3b) amounted to 1.33 for *BP* I and 1.14 for *BP* II. The maxima of the wide-band scattering by the fog phase (Figs. 3a and 4) were located in all structures between the diffraction peaks of *BP* II and those of the cholesteric phase, and their frequency position had the same linear dependence as the diffraction in cubic structures with a long-range translational order. In the case of the fog phases of the structures based on CN we found that the ratio in question was $\lambda_B/\lambda_C \sim 1.06$ (Fig. 3b).

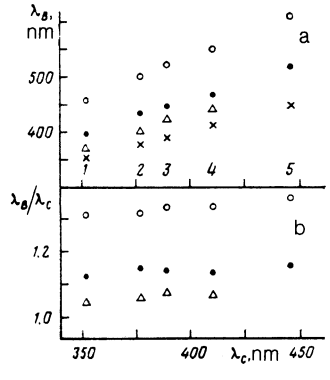

FIG. 3. Dependences of the spectral positions of the long-wavelength reflections λ_B (a) and λ_B/λ_C (b) exhibited by the *BP* I (○), *BP* II (●), and *BP* III (△) phases of CN-CC on λ_C of the cholesteric phase: 1) CN; 2) CN-CC (95:5); 3) CN-CC (93:7); 4) CN-CC (90:10); 5) CN-CC (86:14).

A theory of blue phases[1,9,10] predicts the following relationship between the positions of the diffraction lines in the spectrum and the moduli of the Fourier harmonics $\epsilon^2(\sigma)$ ($\sigma = n^2 + k^2 + l^2$) representing the intensity of diffraction $P_C = \lambda_C/2n \sin\theta$ and $P_B = \lambda_B/2n \sin\theta$:

$$P_C/P_B = \sum_{\sigma} \sigma^{1/2}\epsilon^2(\sigma)/\sigma\epsilon^2(\sigma). \quad (1)$$

Estimates based on Eq. (1) demonstrated that practically the whole intensity of diffraction by the fog phase in structures with the left-handed direction of the twist of the helix was concentrated in the experimentally observed wide-band maximum, i.e., the amplitudes of the higher Fourier harmonics were small, in agreement with the icosahedral model of the fog phase.[11,13] The intensity of diffraction at $\lambda = \lambda_B/2^{1/2}$ could not exceed 12% and at $\lambda = \lambda_B/3^{1/2}$ it should not be more than 5% of the main maximum. The diffraction maximum of the fog phase of CC, which had a right-hand helix twist, was also located on the long-wavelength side of the selective reflection of the cholesteric and was characterized by a large red shift $\lambda_B/\lambda_C \sim 1.14$, compared with the shift in the case of structures with the left-hand helix twist (CN).

The positions of the diffraction maxima in the spectra (Fig. 4) were characterized by a period which agreed with the short-range order in the fog phase P_B and the half-width of the diffraction for a given value of P_B agreed with the correlation length. The large long-wavelength shift of the diffraction in a series of related compounds such as CN and CN-CC mixtures (Fig. 4) made it possible to find the changes in the parameters of disorder associated with an increase in the period of the structure from the experimental data. An analysis of the data was made employing two models of disorder in the fog phase.

1) Discrete polycrystalline model. In this model it is assumed that there is translational order in small arbitrarily oriented crystals. The scattering by neighboring crystallites is assumed to be noncoherent. The diffraction from a liquid crystallite of spherical shape was calculated by Belyakov *et al.*[7]:

$$R \sim \alpha^{-4}(1+\alpha^2 D^2 \varkappa_0^2/2 - \cos\alpha D\varkappa_0 - \alpha D\varkappa_0 \sin\alpha D\varkappa_0), \quad (2)$$

where $\alpha = [\tau^2 + 2(\varkappa_0\tau)]/2\varkappa_0^2$, D is the diameter of the crystallite, τ is the reciprocal lattice vector, and $\varkappa_0$ is the wave vector of the incident wave.

2) Paracrystalline model with a continuous loss of correlation of the translational order. In this model a disordered structure is postulated and this structure is characterized by a Gaussian H_m distribution of the neighboring planes at distances $mP_B + x$:

$$H_m(mP_B+x) = (2\pi m)^{-1/2}\Delta \exp(-x^2/2\Delta_m^2). \quad (3)$$

The interference function of such a structure is of the form[14]

$$Z(X) = (1-|F|^2)/(1-2|F|\cos\chi+|F|^2),$$

where $|F(X)| = \exp(-2\pi^2X^2\Delta^2)$, $\chi^2 = 2\pi XP_B$, $X = 2n\sin\theta/\lambda$. A measure of disorder is the dispersion (scatter) Δ of the distribution function $H(x)$. In the case of the polycrystalline model a measure of disorder is the diameter of a crystal D.

The values of D and Δ were determined by comparing the experimental curves of Fig. 4 with the results of calculations based on Eqs. (2) and (3) (Fig. 5). The fitting was carried out using the half-width of the diffraction maxima (Fig. 5).

The polycrytalline model indicated that the diameter of crystallites was 0.7–1 μ, increasing along the series CN, CC, and CN-CC as the diffraction band of the fog phase shifted toward longer wavelengths. Therefore, the effective distance in which the order was retained in the fog phase increased on increase in the period of the structure. The ratio D/P_B was far too small (~ 6) to regard *BP* III as an ordinary polycrystalline sample consisting of a three-dimensionally ordered blue phase. Such a value of the ratio D/P_B was more typical of clusters in an amorphous sample. Rapid cooling of a liquid crystal CE4 (Ref. 15), which was in blue phase, was reported to cause vitrification of a sample. Cooling from the fog phase in the vitrified (glassy) state produced longish objects of 0.1–1 μ size observed with an electron microscope.[15] Clearly, these objects were associated with the presence of regions of correlated distributions of molecules, of size 0.7–1 μ, observed in the fog phase.

Estimates based on the polycrystalline model predicted a large number of unit cells on the surface of a crystallite ($\sim 70\%$ of their number in the crystallite), i.e., a large part of the volume of the fog phase could be subject to structural distortions. The imperfect translational periodicity of the sample was described well by the paracrystalline model. The spread Δ of the distribution function $H(x)$ of the fog phase was 20–24 nm, which represented 15–18% of P_B, i.e., the short-range order was distorted strongly in just one period of the structure of P_B. The radius of the ordering L, within which a short-range correlation was observed [broadening of $H(x)$ did not exceed the periodicity], deduced from the diffraction measurements, was limited to 0.8–1.2 μ. The parameters of the disorder Δ and P_B, as well as the effective distances in which the order was maintained (D in the polycrystalline model and L in the paracrystalline model) were comparable with the corresponding characteristics of glassy samples.

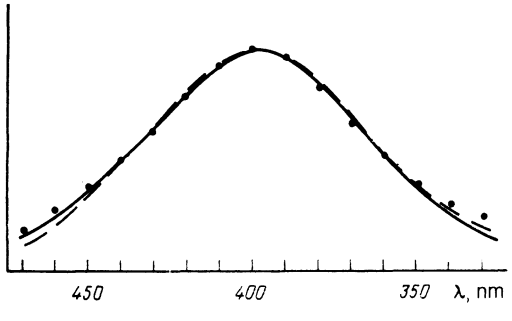

FIG. 5. Diffraction line predicted by the polycrystalline model (dashed curve) and by the paracrystalline model (dots). The actual profile of the wide-band reflection exhibited by the *BP* III phase of CN-CC (95:5) is represented by the continuous curve.

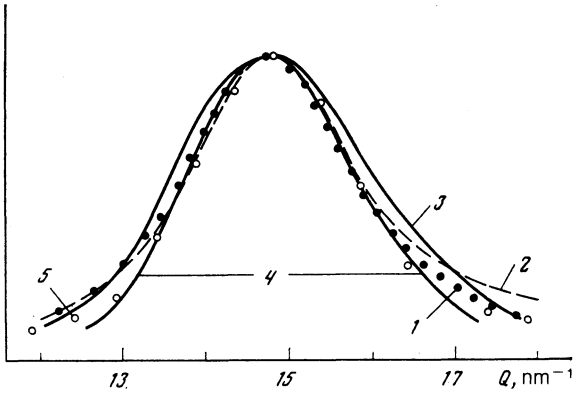

FIG. 6. Neutron[16] (curve 1) and x-ray[17] diffraction by the amorphous phase of MBBA ($Q = 4\pi\sin\theta/\lambda$). Curves 3 and 4 represent, respectively, the diffraction of light by the *BP* III phase of CN (curve 3) and CN-CC (90:10) (curve 4); $Q = Q_BP_B/d$ (see text). Curve 5 represents x-ray diffraction by metallic glass $Ni_{60}Nb_{40}$ (Ref. 18).

Figure 6 shows the neutron[16] and x-ray[17] diffraction patterns of MBBA frozen rapidly to form the glassy state. The diffraction peak was associated with a short-range molecular ordering of the orientations of the long axes of the molecules ($d \sim 0.42$-0.43 nm). In the fog phase the supramolecular order in the orientation of the liquid-crystal director was characterized by a parameter $P_B \sim 120$–150 nm, which was 280–350 times greater than the intermolecular distances in MBBA. A comparison of the neutron and x-ray diffraction patterns in the solid amorphous state with the optical data for *BP* III was made in Fig. 6 plotting the results of diffraction in the fog phase on a scale enlarged along the horizontal axis ($Q = Q_BP_B/d$). We also plotted in the same figure the structure factor of the main diffraction peak $Q = 29.45\ \text{nm}^{-1}$ of metallic glass $Ni_{60}Nb_{40}$ deduced from x-ray diffraction.[18] The data for this metallic glass[18] were plotted in Fig. 6 on a scale reduced along the Q axis in order to equalize the periods of the short-range order in the metallic glass, in MBBA, and in *PB* III. It is clear from Fig. 6 that the half-widths of the diffraction peaks of the fog phase, MBBA, and metallic glass were practically identical. The similarity of the diffraction in *BP* III, MBBA, and $Ni_{60}Nb_{40}$ led us to the conclusion that a glassy-type disorder was characteristic of the fog phase. In solids such a disorder was observed in nonequilibrium phases (glass, amorphous state), whereas *BP* III is a phase in thermodynamic equilibrium.

There is an analogy in the possible method of description of the structure of solid-state glasses and of the cubic

BP I and *BP* II phases[19]: in glasses the short-range order in the distribution of atoms may be incompatible with the crystalline order and the contact between ordered regions is via structure defects. In the cubic liquid crystal phases the double twist of the director field means that a fairly large volume cannot be filled without formation of singularities (disclinations).[20-22] The distribution of defects in *BP* I and *BP* II are ordered, forming a cubic structure of a disclination lattice. The phase transition from the cubic to the fog phase may involve disordering of defects (disclinations). The relative volume of defects in *BP* I (Ref. 22) is $V_{\text{core}} = 6\pi r^2/d^2$, where $r \sim 0.04d$ ($d \sim 250$ nm is the cell parameter and r is the radius of a disclination core). If we assume that in the fog phase these defects are located on the surfaces of disordered regions, the relative volume of disclinations and their cross sections can be used to estimate the size of ordered regions in *BP* III. This gives the radius of the ordered regions $R \approx 3r/V_{\text{core}} \approx 1\ \mu$, which is close to the size of crystallites deduced by us from the experimental data ($D \sim 1\ \mu$, $2L \sim 2\ \mu$). The increase in energy because of the presence of defects is compensated by the reduction due to the ordering inside the cluster, which is the reason for the thermodynamic stability of *BP* III.

The optical diffraction studies show that the fog phase is qualitatively different from other liquid crystal phases whose structure is at present well understood. In the case of nematics, cholesterics, smectics *A*, *C*, *C* *, *D* etc., the order of a structure (orientational or translational) is conserved over macroscopic distances. In the fog phase the ordered regions are comparable with the effective period. A similar situation occurs in liquid crystals in the pretransition region, for example, in the nematic phase, when at temperatures 10 °C before the transition to the smectic *A* phase the correlation length ξ of the translational smectic ordering with a period d is comparable with d ($\xi \sim 5d$). However, in this case the local ordering is of fluctuation nature and appears in a less ordered phase without a phase transition, whereas ordering in the fog phase is of structural nature and occurs as a result of a phase transition. The numerous investigations of liquid crystals proceeding at present will soon allow us to determine whether there are any other liquid crystal phases with finite (like that in *BP* III) ordered regions.

The authors are grateful to V. A. Belyakov, V. E. Dmitrienko, and D. E. Khmel'nitskiĭ for valuable discussions.

[1]V. A. Belyakov and V. E. Dmitrienko, Usp. Fiz. Nauk **146**, 369 (1985) [Sov. Phys. Usp. **28**, 535 (1985)].
[2]H. Stegemeyer T. Blumel, K. Hiltrop, H. Onusseit, and F. Porsch, Liq. Cryst. **1**, 3 (1986).
[3]S. Meiboom and M. Sammon, Phys. Rev. Lett. **44**, 882 (1980); Phys. Rev. A **24**, 468 (1981).
[4]D. L. Johnson, J. H. Flack, and P. P. Crooker, Phys. Rev. Lett. **45**, 641 (1980).
[5]V. A. Kizel' and V. V. Prokhorov, Zh. Eksp. Teor. Fiz. **87**, 450 (1984) [Sov. Phys. JETP **60**, 257 (1984)].
[6]P. J. Collings, Phys. Rev. A **30**, 1990 (1984).
[7]V. A. Belyakov, E. I. Demikhov, V. E. Dmitrienko, and V. K. Dolganov, Zh. Eksp. Teor. Fiz. **89**, 2035 (1985) [Sov. Phys. JETP **62**, 1173 (1985)].
[8]E. I. Demikhov, V. K. Dolganov, and S. P. Krylova, Pis'ma Zh. Eksp. Teor. Fiz. **42**, 15 (1985) [JETP Lett. **42**, 16 (1985)].
[9]H. Kleinert, Phys. Lett. A **81**, 141 (1981).
[10]H. Grebel, R. M. Hornreich, and S. Shtrikman, Phys. Rev. A **28**, 1114 (1983); **30**, 3264 (1984).
[11]R. M. Hornreich and S. Shtrikman, Phys. Rev. Lett. **56**, 1723 (1986).
[12]D. S. Rokhsar and J. P. Sethna, Phys. Rev. Lett. **56**, 1727 (1986).
[13]V. M. Filev, Pis'ma Zh. Eksp. Teor. Fiz. **43**, 523 (1986) [JETP Lett. **43**, 677 (1986)].
[14]B. K. Vaĭnshteĭn, Diffraction of X Rays by Chain Molecules [in Russian], Izd. AN SSSR, Moscow (1963), p. 371.
[15]J. A. N. Zasadzinski, S. Meiboom, M. J. Sammon, and D. W. Berreman, Phys. Rev. Lett. **57**, 364 (1986).
[16]V. K. Dolganov, N. Kroo, L. Rosta, and E.F Sheka, Mol. Cryst. Liq. Cryst. Lett. **64**, 115 (1980).
[17]V. K. Dolganov, L. A. Novomlinskiĭ, and I. M. Shmyt'ko, Fiz. Tverd. Tela (Leningrad) **23**, 2427 (1981); **24**, 2605 (1982) [Sov. Phys. Solid State **23**, 1418(1981); **24**, 1476 (1982)].
[18]E. Svab, F. Forgacs, F. Hajdu, N. Kroo, and J. Takacs, J. Non-Cryst. Solids **46**, 125 (1981).
[19]J. P. Sethna, Phys. Rev. Lett. **51**, 2198 (1983).
[20]S. Meiboom, J. P. Sethna, P. W. Anderson, and W. F. Brinkman, Phys. Rev. Lett. **46**, 1216 (1981).
[21]R. M. Hornreich, M. Kugler, and S. Shtrikman, Phys. Rev. Lett. **48**, 1404 (1982).
[22]S. Meiboom, M. Sammon, and W. F. Brinkman, Phys. Rev. A **27**, 438 (1983).

Translated by A. Tybulewicz